Sensor Configuration and Activation for Field Detection in Large Sensor Arrays

Youngchul Sung and Lang Tong
School of Electrical and Computer Engineering
Cornell University
Ithaca, NY 14850, USA
Email:{ys87,ltong}@ece.cornell.edu

H. Vincent Poor
Dept. of Electrical Engineering
Princeton University
Princeton, NJ 08544
Email:poor@princeton.edu

***Abstract*— The problems of sensor configuration and activation for the detection of correlated random fields using large sensor arrays are considered. Using results that characterize the large-array performance of sensor networks in this application, the detection capabilities of different sensor configurations are analyzed and compared. The dependence of the optimal choice of configuration on parameters such as sensor signal-to-noise ratio (SNR), field correlation, etc., is examined, yielding insights into the most effective choices for sensor selection and activation in various operating regimes.**

I. INTRODUCTION

The main design criteria for sensor networks are the performance in the specific task and the energy efficiency of the network. In this paper, we consider optimal sensor configuration and selection for densely deployed sensor networks for the detection of correlated random fields. An example in which the problem of such sensor selection arises is Sensor Network with Mobile Access (SENMA), as shown in Fig. 1, where a mobile access point collects sensor data controlling sensor transmissions in the reachback channel. To maximize

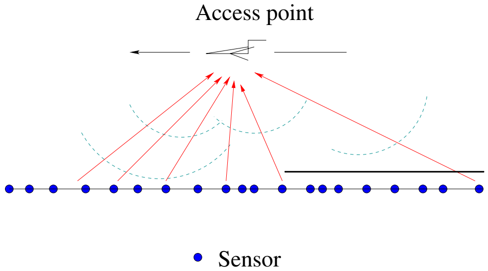

Fig. 1. Sensor network with mobile access point

the energy efficiency of such a network, one should judiciously select and activate sensors to satisfy the desired detection performance with the minimum amount of sensor data since the number of activated sensors is directly related to the energy consumption of the entire network.

To simplify the problem for analysis, we focus on a 1-dimensional space, and investigate how various parameters such as the field correlation, signal-to-noise ratio (SNR), etc., affect the optimal configuration for different sensor schedules. Specifically, we assume that the signal field $s(x)$ is the stationary solution of the stochastic diffusion equation [3]:

$$\frac{ds(x)}{dx} = -As(x) + Bu(x), \quad x \geq 0, \tag{1}$$

where $A \geq 0$ and B are known, and the initial condition is given by $s(0) \sim \mathcal{N}(0, \Pi_0)$. Here, x denotes position along the linear axis of the sensor array. The process noise $u(x)$ is a zero-mean white Gaussian process, independent of both sensor measurement noises $\{w_i\}$ and the initial state $s(0)$. We assume that each activated sensor takes a measurement of the field at its location, and subsequently transmits the data to the collector or fusion center[1]. The observation y_i from the activated sensor i located at x_i ($x_i < x_{i+1}$) is governed by the following statistical hypotheses

$$\begin{array}{lll} H_0 & : & y_i = w_i, \quad i = 1, 2, \cdots, n, \\ H_1 & : & y_i = s_i + w_i, \end{array} \tag{2}$$

where $\{w_i\}$ are $\mathcal{N}(0, \sigma^2)$ measurement noises, with known σ^2 and independent from sensor to sensor, and the signal sample $s_i \triangleq s(x_i)$. The dynamics of the collected signal samples $\{s_i\}$ are given by

$$s_{i+1} = a_i s_i + u_i, \tag{3}$$

$$a_i = e^{-A\Delta_i}, \tag{4}$$

where $\Delta_i \triangleq |x_{i+1} - x_i|$ and $u_i \sim \mathcal{N}(0, \Pi_0(1 - a_i^2))$. A similar model was derived in [4].

Note that $0 \leq a_i \leq 1$ for $0 \leq A \leq \infty$ and a_i determines the amount of correlation between sample s_i and s_{i+1}; $a_i = 0$ implies that two samples are independent while for perfectly correlated signal samples we have $a_i = 1$. By the stationarity, $\mathbb{E}\{s_i^2\} = \Pi_0$ for all i, and the SNR for the observations is given by Π_0/σ^2.

A. Summary of Results

We adopt the Neyman-Pearson formulation of fixing the detector size α and minimizing the miss probability. The miss probability $P_M(\mathcal{X}, n; \alpha, \text{SNR})$ is a function of the number, n, and locations, $\mathcal{X} \triangleq \{x_1, \cdots, x_n\}$, of the activated sensors as well as detector size α and SNR. Usually, the miss probability decreases exponentially as n increases and the error exponent is defined as the decay rate

$$K_\alpha(\mathcal{X}; \text{SNR}) = \lim_{n\to\infty} \frac{1}{n} \log P_M(\mathcal{X}, n; \alpha, \text{SNR}). \tag{5}$$

The error exponent is a good performance index since it gives an estimate of the number of samples required for a given detection performance; faster decay rate implies that fewer samples are needed

This work was supported in part by the Multidisciplinary University Research Initiative (MURI) under the Office of Naval Research Contract N00014-00-1-0564. Prepared through collaborative participation in the Communications and Networks Consortium sponsored by the U. S. Army Research Laboratory under the Collaborative Technology Alliance Program, Cooperative Agreement DAAD19-01-2-0011.

The work of H. V. Poor was supported in part by the Office of Naval Research under Grant N00014-03-1-0102.

[1]We will not focus on local quantization of y_i at the sensor level here, nor will we consider the transmission error to the fusion center. These are important design issues that must be treated separately.

for a given miss probability. Hence, the energy efficient configuration for activation can be formulated to find the optimal $\mathcal{X}$ (where data should be collected) maximizing the error exponent when the sample size is sufficiently large.

Based on our previous results on the behavior of the error exponent for the detection of correlated random fields [17], we examine several strategies for sensor configuration for the testing of H_1 versus H_0, and propose guidelines for the optimal configuration for different operating regimes. Specifically, we consider uniform configuration, periodic clustering, and periodic configuration with arbitrary sensor locations within a period. We show that the optimal configuration is a function of the field correlation and the SNR of the observations. For uniform configuration, the optimal strategy is to cover the entire signal field with the activated sensors for SNR > 1. For SNR < 1, on the other hand, there exists an optimal spacing between the activated sensors. We also derive the error exponents of periodic clustering and arbitrary periodic configurations. Depending on the field correlation and SNR, the periodic clustering outperforms uniform configuration. Furthermore, there exists an optimal cluster size for intermediate values of field correlation. The closed-form error exponent obtained for the vector state-space model explains the transitory error behavior for different sensor configurations as the field correlation changes. It is seen that the optimal periodic configuration is either periodic clustering or uniform configuration for highly correlated or almost independent signal fields.

B. Related Work

The detection of Gauss-Markov processes in Gaussian noise is a classical problem. See [5] and references therein. Our work is based on the large deviations results in [17], where the closed-form error exponent was derived for the Neyman-Pearson detection, with a fixed size, of correlated random fields using the innovations approach for the log-likelihood ratio (LLR) [6]. There is an extensive literature on the large deviation approach to the detection of Gauss-Markov processes [8]-[14]. The application of the large deviations principle (LDP) to sensor networks has been considered by other authors as well. The sensor configuration problem can be viewed as a sampling problem. To this end, Bahr and Bucklew [10] optimized the exponent numerically under a Bayesian formulation. For a specific signal model (low pass signal in colored noise), they showed that the optimal sampling depends on SNR, which we also show in this paper in a different setting. Chamberland and Veeravalli have also considered the detection of correlated fields in large sensor networks under the formulation of LDP and a fixed threshold for the LLR test with the focus on detection performance under power constraint [16].

II. Preliminaries: Error Exponent and Properties

In this section we briefly present previous results [17] relevant to our sensor configuration problem. The error exponent for the Neyman-Pearson detection of the hypotheses (2) with a fixed size $\alpha \in (0,1)$ and uniformly configured sensors with spacing Δ (i.e., $\mathcal{X} = \{(i-1)\Delta\}_{i=1}^{n}$) is given by

$$K_\alpha(\mathcal{X};\mathrm{SNR}) = -\frac{1}{2}\log\frac{\sigma^2}{R_e} + \frac{1}{2}\frac{\tilde{R}_e}{R_e} - \frac{1}{2}, \qquad (6)$$

independently of the value of α, where R_e and $\tilde{R}_e$ are the steady-state variances of the innovations process of $\{y_i\}$ calculated under H_1 and H_0, respectively. The closed-form formula (6) is obtained via the innovations representation of the log-likelihood ratio [6], and enables us to further investigate the properties of the error exponent with respect to (w.r.t.) parameters such as the correlation strength and SNR. (See [17] for more detail.) Here, we note that the error exponent for the miss probability with a fixed size does not depend on the value α of the size. Thus, the error exponent depends only on $\mathcal{X}$ and SNR. (For notational convenience, we use K for the error exponent unless the arguments are needed.)

We now describe the basic properties of the error exponent starting from the extreme correlation cases.

Theorem 1 (Extreme correlations): The error exponent K is a continuous function of the correlation coefficient $a \triangleq e^{-A\Delta}$ for a given SNR. Furthermore,

(i) for i.i.d. observations ($a = 0$) the error exponent K reduces to the Kullback-Leibler information $D(p_0||p_1)$ where $p_0 \sim \mathcal{N}(0,\sigma^2)$ and $p_1 \sim \mathcal{N}(0,\Pi_0+\sigma^2)$;
(ii) for the perfectly correlated signal ($a = 1$) the error exponent K is zero for any SNR, and the miss probability decays to zero with $\Theta(\frac{1}{\sqrt{n}})$.

The above theorem reduces to the Stein's lemma for the i.i.d. case. For the perfectly correlated case ($a = 1$), on the other hand, the miss probability does not decay exponentially; rather it decays in polynomial order $n^{-1/2}$.

The error behavior for intermediate values of correlation is summarized by the following theorem, and shows distinct characteristics for different SNR regimes.

Theorem 2 (K vs. correlation): (i) For SNR > 1, K decreases monotonically as the correlation increases (i.e. $a \uparrow 1$);
(ii) For SNR < 1, there exists a non-zero correlation value a^* that achieves the maximal K, and a^* is given by the solution of the following equation.

$$[1 + a^2 + \Gamma(1-a^2)]^2 - 2(r_e + \frac{a^4}{r_e}) = 0, \qquad (7)$$

where $r_e = R_e/\sigma^2$. Furthermore, a^* converges to one as SNR approaches zero.

Hence, an i.i.d. signal gives the best detection performance for a given SNR > 1. The intuition behind this result is that the signal component in the observation is strong at high SNR, and the new information contained in the observation provides more benefit to the detector than the noise averaging effect present for correlated observations. For SNR < 1, on the other hand, the error exponent does not decrease monotonically as correlation becomes strong, and there exists an optimal correlation. This is because at low SNR the signal component is weak in the observation and correlation between signal samples provides a noise averaging effect. This noise averaging will become evident in Section III-B. Fig. 2 shows the error exponent as a function of the correlation coefficient a for several values of SNR. Two plots clearly show the different error behaviors as a function of correlation

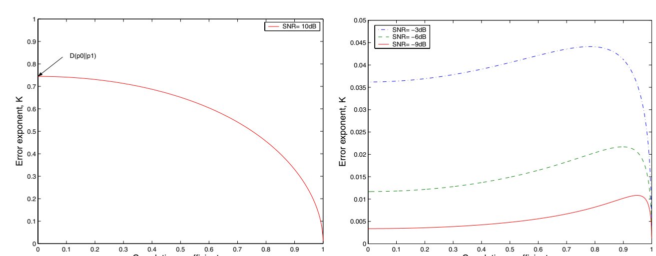

(a) (b)

Fig. 2. K vs. correlation coefficient a: (a) SNR = 10 dB (b) SNR= -3, -6, -9 dB

in the high and low SNR regimes. Unit SNR is a transition point between two different behavioral regimes of the error exponent as a function of correlation strength.

The error exponent is also a function of SNR. This aspect of the behavior of the error exponent is given by the following theorem.

Theorem 3 (K vs. SNR): The error exponent K is monotone increasing as SNR increases for a given correlation coefficient $0 \le a < 1$. Moreover, at high SNR the error exponent K increases linearly with respect to $\frac{1}{2}\log \text{SNR}$.

III. Sensor Configuration

In this section, we investigate several sensor configurations, and analyze the corresponding detection performance via the error exponent. We also provide the closed-form error-exponent for several interesting cases by extending the results in the previous section. Specifically, we consider uniform configuration, clustering, and periodic configuration with arbitrary locations within a spatial period as described in Fig. 3. We provide the optimal configuration for uniform configuration for the detection of stationary correlated fields, and investigate the benefit of other configurations.

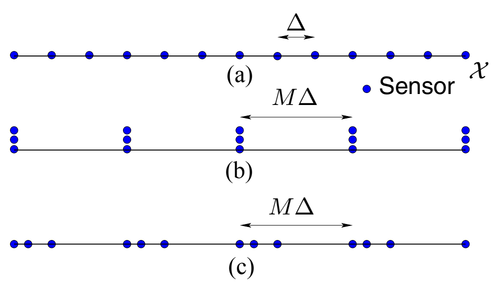

Fig. 3. Configurations for n sensor activations: (a) uniform configuration (b) periodic clustering (c) arbitrary periodic configuration

A. Uniform Configuration

For uniform configuration with spacing Δ between neighboring sensors, the data model is described by the state-space model (3) with

$$a_1 = \cdots = a_n = a = e^{-A\Delta},$$

and the results in Section II are directly applicable. The key connection between sensor configuration and detector performance is given by the correlation coefficient a. First, we consider SNR > 1. In this case, by Theorem 2 *(i)*, the error exponent decreases monotonically as a increases, i.e., the spacing Δ decreases for a given field diffusion rate A. Hence, when the support of the signal field $\mathcal{S}$ is finite and n sensors are planned to be activated in the field, the optimal uniform scheme is to distribute the n activated sensors to cover all the signal field, which makes the observations least correlated; localizing all the scheduled sensors in a subregion of the stationary signal field is not optimal. For SNR < 1, on the other hand, the optimal spacing Δ^* for an infinite (in size) signal field is given by

$$\Delta^* = -\log \frac{a^*}{A}, \tag{8}$$

where a^* is given by the solution of (7). Δ^* is finite for any SNR strictly less than one since the diffusion coefficient $A < 0$ and $a^* > 0$ for any SNR < 1. The optimal spacing as a function of SNR is shown for $A = 1$ in Fig. 4.

For a finite signal field $\mathcal{S}$ with n scheduled sensors, Δ^* is still optimal among the class of uniform configurations if $n\Delta^* < |\mathcal{S}|$, where $|\mathcal{S}|$ is the spatial duration of the signal field. In this case, the sensor field does not need to cover the entire signal field. However, if $n\Delta^* > |\mathcal{S}|$, Δ^* may no longer be the optimal spacing. As shown in Fig. 2, the error exponent decreases when the spacing Δ deviates from Δ^*. Hence, activating sensors fewer than $\bar{n} \triangleq \lfloor \frac{|\mathcal{S}|}{\Delta^*} \rfloor$ with spacing larger than Δ^* always gives a worse performance than $\bar{n}$ sensors with spacing Δ^*. However, this may not be the case for activating more sensors than $\bar{n}$ (up to n) by reducing the spacing from Δ^*. Even if the error exponent decreases by reducing the spacing, more sensors are activated over the signal field. Therefore, better performance is possible for the latter case since the product of the error exponent and the number of samples determines the miss probability approximately. Similar situation also occurs at SNR > 1 for finite signal field. Note that the error exponent increases as the correlation decreases. (See Fig. 2.) Thus, by spreading the activated sensors with a reduced number of activated sensors in the signal field, sensor data become less correlated and the slope of error decay becomes larger at a cost of reducing the number of observations. However, the increase in the error exponent is not large enough to compensate for the loss in the number of sensors in the field. Fig. 5 shows the error exponent as a function of the number of scheduled sensors in $\mathcal{S}$ ($|\mathcal{S}| = 1$) at 10 dB SNR for several different diffusion rates. The dashed line shows the decay of n^{-1} for which the performance loss by the decrease in the number of scheduled sensors is exactly balanced. We observe that the decay of the actual error exponent is slower than n^{-1}. Hence, when the maximum number of available sensors in a finite signal field case is n, the optimal configuration is to activate all n sensors covering the entire field with maximal spacing.

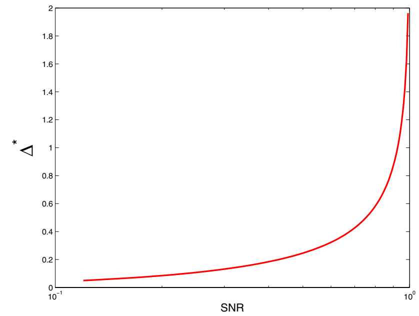

Fig. 4. Optimal spacing between sensors for infinite signal field (SNR < 1, $A = 1$)

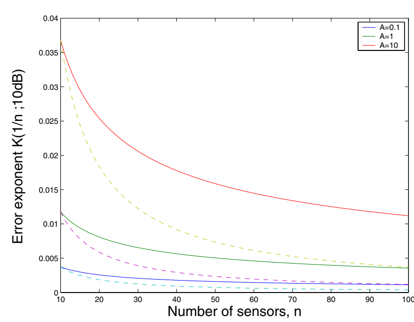

Fig. 5. Error exponent vs. n for a fixed signal field ($|\mathcal{S}| = 1$)

Another interesting fact about the finite signal field is the asymptotic behavior when the number of sensors increases without bound.

In this case, the correlation coefficient converges to one, i.e.,

$$a = \exp\left(-A\frac{|\mathcal{S}|}{n}\right) \to 1 \quad \text{as } n \to \infty. \tag{9}$$

By Theorem 1 *(ii)*, the error probability does not decay exponentially, but decays with polynomial order $n^{-1/2}$ for any finite A as $n \to \infty$. The exception is the singular case where $A = \infty$, i.e., the signal is a white process. Therefore, for the detection of stationary correlated fields, it is a better strategy to cover a larger area as long as the signal field extends there than to localize activated sensors more densely in a subregion.

B. Periodic Clustering

The uniform configuration for a finite signal field reveals that there is a benefit at high SNR to making sensor spacing large to obtain less correlated observations, but activating fewer sensors results in a bigger loss than the gain from being less correlated. This naturally leads to our second configuration: periodic clustering shown in Fig. 3 (b), aiming at the benefits from both correlation and the number of scheduled sensors. In this configuration, we activate M sensors very close in location, and repeat this multiple activation periodically over signal field so that the number of scheduled sensors is preserved and the spacing between clusters becomes larger than that of uniform configuration.

For further analysis, we assume that the M sensors within a cluster are located at the same position. With the total number of scheduled sensors $n = MN$, the observation vector $\mathbf{y}_n = [y_1, y_2, \cdots, y_n]^T$ under H_1 is given by

$$\mathbf{y}_n = \tilde{\mathbf{s}}_n \otimes \mathbf{1}_M + \mathbf{w}_n, \tag{10}$$

where $\otimes$ is the Kronecker product,

$$\tilde{\mathbf{s}}_n = [s(0), s(\tilde{\Delta}), \cdots, s(N\tilde{\Delta})]^T, \tag{11}$$

and $\tilde{\Delta} = |\mathcal{S}|/N = M\Delta$. ($\Delta$ is the sensor spacing for the uniform configuration for n sensors in $\mathcal{S}$.) The covariance matrix of $\mathbf{y}_n$ is given by

$$\mathbb{E}\{\mathbf{y}_n\mathbf{y}_n^T\} = \begin{cases} \Sigma_{s,N}(\tilde{a}) \otimes \mathbf{1}_M\mathbf{1}_M^T + \sigma^2\mathbf{I} & \text{under } H_1, \\ \sigma^2\mathbf{I} & \text{under } H_0, \end{cases} \tag{12}$$

where $\tilde{a} = \exp(-A\tilde{\Delta})$. The signal covariance matrix has a block Toeplitz structure due to the perfect correlation of signal samples within a cluster. $\mathbf{\Sigma}_{s,N}(\tilde{a})$ in (12) is a positive-semidefinite Toeplitz matrix where the kth off-diagonal entries are given by $r_s(k) = \Pi_0\tilde{a}^k$. For any $A > 0$, $0 \le \tilde{a} < 1$ and $r_s(\cdot)$ is an absolutely summable sequence; the eigenvalues of $\mathbf{\Sigma}_{s,n}$ are bounded from above and below[7]. Using the convergence of the eigenvalues of $\mathbf{\Sigma}_{s,N}$ and the properties of the Kronecker product, we obtain the error exponent for periodic clustering.

Proposition 1 (Periodic Clustering): For the Neyman-Pearson detector for the hypotheses (2) with level $\alpha \in (0,1)$ and periodically clustered sensor configuration, the error exponent of the miss probability is given by

$$\tilde{K} = \frac{1}{M}K(\tilde{\Delta}; M * \text{SNR}), \tag{13}$$

where $K(\tilde{\Delta}; M * \text{SNR})$ is the error exponent for uniform configuration with spacing $\tilde{\Delta}$ and $M * \text{SNR}$ for each sensor.

Proof: See [18].

The optimal detector for periodic clustering consists of two steps. We first take an average of the observations within each cluster, and then apply the optimal detector for a single sample at each location to the ensemble of N average values. Intuitively, it is reasonable to average the observations within a cluster since the signal component is in the same direction and the noise is random. By averaging, the magnitude of the signal component increases by M times with the increase in the noise power by the same factor; the SNR within a cluster increases by the factor M. This is shown in the relation (13) to uniform configuration. The error exponent (13) shows the advantage and disadvantage of the periodic clustering over uniform configuration covering the same signal field. Clustering gives two benefits. First, the correlation between clusters is reduced for the same A by making the spacing larger, and the error decay per cluster increases. Second, the SNR for each cluster also increases by M times. However, the effective number of signal samples is also reduced by a factor of M comparing with the uniform configuration. The performance of clustering is determined by the dominating factor depending on the diffusion rate of the underlying signal and the SNR of the observations. Fig. 6 shows $\exp(-n\tilde{K})$, which is an

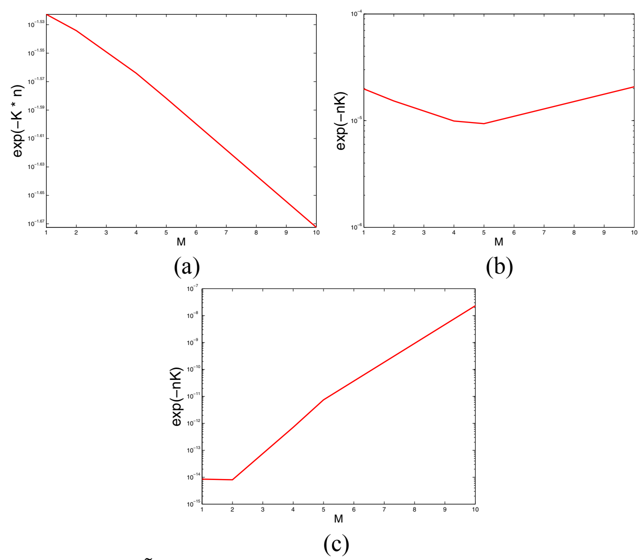

Fig. 6. $\exp(-n\tilde{K})$ vs. M ($|\mathcal{S}| = 1$, SNR = 10 dB): (a) $A = 0.1$ (b) $A = 1$ (c) $A = 10$

approximate miss probability for large samples, for different diffusion rates at 10 dB SNR. The total number of sensors is fixed at $n = 100$, and the cluster size is chosen as $M = [1, 2, 4, 5, 10]$. For the highly correlated field ($A = 0.1$), it is seen that the reduced correlation between sampled signals is dominant and the periodic clustering gives better performance than uniform configuration (i.e., $M = 1$). (See Fig. 2. The gain in the error exponent due to reducing correlations is large in the high correlation region.) On the other hand, for the almost independent signal field ($A = 10$), clustering gives worse performance than uniform configuration. In this case, the correlation between the scheduled samples is already weak, and the increase in the error exponent due to increased spacing is insignificant as shown in Fig. 2. Hence, the benefit of clustering results only from the increase in SNR. By Theorem 3, however, the rate of increase in the error exponent due to the increased SNR is $\frac{1}{2}\log M$ at high SNR, which does not compensate for the loss in the number of effective samples by the factor $1/M$. For the signal field with intermediate correlation, there is a trade-off between the gain and loss of clustering, and there exists an optimal clustering as shown in Fig.6 (b). Hence, one should choose the optimal clustering depending on the diffusion rate and the size of the underlying signal field. Fig. 7 shows the

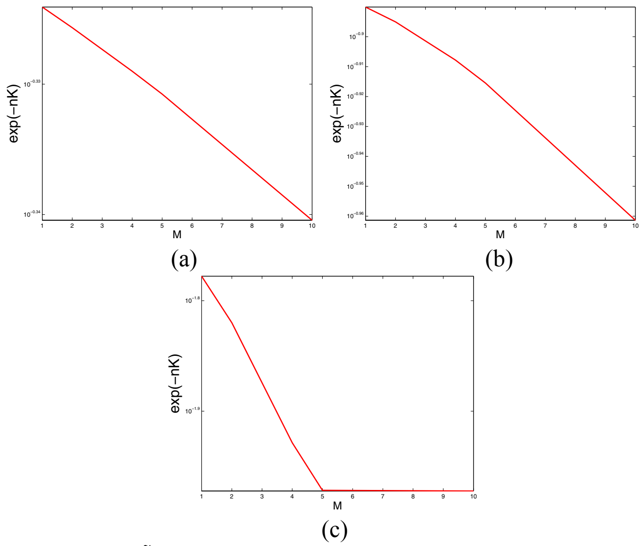

Fig. 7. $\exp(-n\tilde{K})$ vs. M ($|\mathcal{X}| = 1$, SNR = -3 dB): (a) $A = 0.1$ (b) $A = 1$ (c) $A = 10$

approximate miss probability of the periodic clustering for -3 dB SNR with other parameters the same as in the high SNR case. It is seen that periodic clustering outperforms than uniform configuration in all considered correlation values since the SNR is the dominant factor in the detector performance at low SNR.

Clustering also explains the polynomial behavior in asymptotic error decay for the infinite density model considered in (9). We can view an increase in the number n of sensors in a finite signal field as increasing the cluster size M with a fixed number N of clusters. As n increases, SNR per cluster increases linearly with n, and will be in the high SNR regime eventually. At high SNR, the error exponent increases at the rate of $\frac{1}{2}\log \text{SNR}$ by Theorem 3. Hence, the overall miss probability is given approximately by

$$P_M \approx C\exp(-NK) = C_1\exp(-\frac{1}{2}N\log n) \sim C_2 n^{-1/2}, \quad (14)$$

for sufficiently large n, which coincides the results in Theorem 1 *(ii)*. Now it is clear that for highly correlated cases the decay in error probability with an increasing number of sensors is mainly due to the noise averaging effect rather than the effect of the new information about the signal in the observations.

C. Arbitrary Periodic Configuration

The previous section shows that periodic clustering outperforms uniform configuration depending on the field correlation. However, periodic clustering is limited since all the sensors within a spatial period are scheduled on the same location. Considering periodic structure we now generalize the locations of the scheduled sensors within a period. First, we provide the closed-form error exponent for the Neyman-Pearson detector for stationary vector Gauss-Markov signals using noisy sensors. Using the closed-form error exponent, we investigate the optimal periodic configuration with arbitrary locations within a period.

We again consider $n = MN$ sensors scheduled over $\mathcal{S}$ with M sensors within a period, and denote the relative distance of M sensors within a period as

$$x_1 = 0,\ x_2 - x_1 = \Delta_1,\ x_3 - x_2 = \Delta_2,\ \cdots, x_{M+1} - x_M = \Delta_M.$$

Hence, the interval of a period is $\Delta = \Delta_1 + \cdots + \Delta_M$. Define the signal sample and observation vectors for period i as

$$\vec{s}_i \triangleq [s_{1i}, s_{2i}, \cdots, s_{Mi}]^T, \quad i = 1, \cdots, N, \quad (15)$$

$$\vec{y}_i \triangleq [y_{1i}, y_{2i}, \cdots, y_{Mi}]^T, \quad (16)$$

where $s_{mi} = s_{(i-1)M+m}$ and $y_{mi} = y_{(i-1)M+m}$. The hypotheses (2) can be rewritten in vector form as

$$\begin{array}{lll} H_0 & : & \vec{y}_i = \vec{w}_i, \qquad i = 1, 2, \cdots, N, \\ H_1 & : & \vec{y}_i = \vec{s}_i + \vec{w}_i, \end{array} \quad (17)$$

where the measurement noise $\vec{w}_i \sim \mathcal{N}(\mathbf{0}, \sigma^2\mathbf{I}_M)$ independent over i, and $\vec{s}_i$ satisfies the vector state-space model

$$\begin{array}{rcl} \vec{s}_{i+1} & = & \mathbf{A}\vec{s}_i + \mathbf{B}\vec{u}_i, \\ \vec{u}_i & \stackrel{i.i.d.}{\sim} & \mathcal{N}(0,\ \mathbf{Q}), \quad \mathbf{Q} \geq 0, \end{array} \quad (18)$$

where $\vec{u}_i$ are defined similarly to the quantities in (15). Specifically, the feedback and input matrices, $\mathbf{A}$ and $\mathbf{B}$, are given from the scalar state-space model as

$$\mathbf{A} = \begin{bmatrix} 0 & 0 & 0 & e^{-A\Delta_M} \\ 0 & 0 & 0 & e^{-A(\Delta_M+\Delta_1)} \\ & & & \vdots \\ 0 & 0 & 0 & \\ 0 & 0 & 0 & e^{-A(\Delta_M+\Delta_1+\cdots+\Delta_{M-1})} \end{bmatrix}, \quad (19)$$

and

$$\mathbf{B} = \begin{bmatrix} 1 & 0 & 0 & 0 \\ e^{-A\Delta_1} & 1 & 0 & 0 \\ \vdots & \cdots & \ddots & 0 \\ e^{-A(\Delta_1+\cdots+\Delta_{M-1})} & & e^{-A\Delta_{M-1}} & 1 \end{bmatrix}, \quad (20)$$

and

$$\mathbf{Q} = \Pi_0 \text{diag}((1 - e^{-2A\Delta_M}), (1 - e^{-2A\Delta_1}), \cdots, (1 - e^{-2A\Delta_{M-1}})).$$

Notice that $\mathbf{A}$, $\mathbf{B}$, and $\mathbf{Q}$ are not varying with i due to the periodicity. Only the last column of $\mathbf{A}$ is non-zero due to the Markov property of the scalar process $\{s_i\}$, and the corresponding non-zero eigenvalue of $\mathbf{A}$ is simply given by $\lambda = e^{-A\Delta}$ so that $|\lambda| < 1$ for arbitrary sensor locations within a period for any diffusion rate $A > 0$. Notice that the eigenvalue is the same as the correlation coefficient a with sampling distance Δ, the period of the interval. The initial condition for the vector model is given by

$$\vec{s}_1 \sim \mathcal{N}(0, \mathbf{C}_0), \quad (21)$$

where $\mathbf{C}_0$ is given by

$$\Pi_0 \begin{bmatrix} 1 & e^{-A\Delta_{1,2}} & e^{-A\Delta_{1,3}} & \cdots & e^{-A\Delta_{1,M}} \\ e^{-A\Delta_{2,1}} & 1 & e^{-A\Delta_{2,3}} & & e^{-A\Delta_{2,M}} \\ e^{-A\Delta_{3,1}} & e^{-A\Delta_{3,3}} & 1 & e^{-A\Delta_{3,4}} & \vdots \\ \vdots & & & \ddots & e^{-A\Delta_{1,M-1}} \\ e^{-A\Delta_{M,1}} & \cdots & & e^{-A\Delta_{M-1,1}} & 1 \end{bmatrix},$$

and $\Delta_{i,j} \triangleq |x_j - x_i|$. The initial covariance matrix $\mathbf{C}_0$ is derived from the scalar initial condition $s_1 \sim \mathcal{N}(0, \Pi_0)$, and it can be shown that $\mathbf{C}_0$ satisfies the following Lyapunov equation

$$\mathbf{C}_0 = \mathbf{A}\mathbf{C}_0\mathbf{A}^T + \mathbf{B}\mathbf{Q}\mathbf{B}^T. \quad (22)$$

Thus, the vector signal sequence $\{\vec{s}_i\}$ is a stationary process although the scalar process is not in general for the arbitrary periodic configuration.

For the vector case, the innovations approach [17] to obtain the error exponent is very useful, and provides a closed-form formula for the error exponent of the Neyman-Pearson detection of stationary vector processes in noisy observations.

Proposition 2 (Arbitrary Periodic Configuration): For the Neyman-Pearson detector for the hypotheses (17,18) with level $\alpha \in (0,1)$ (i.e. $P_F \leq \alpha$), the best error exponent of the miss probability (per a vector observation) is given by

$$K_v = -\frac{1}{2}\log\frac{\sigma^{2m}}{det(\mathbf{R}_e)} + \frac{1}{2}\text{tr}\left(\mathbf{R}_e^{-1}\tilde{\mathbf{R}}_e\right) - \frac{m}{2}, \tag{23}$$

independently of the value of α. The steady-state covariance matrices $\mathbf{R}_e$ and $\tilde{\mathbf{R}}_e$ of the innovation process calculated under H_1 and H_0, respectively, are given by

$$\mathbf{R}_e = \sigma^2\mathbf{I}_m + \mathbf{P}, \tag{24}$$

where $\mathbf{P}$ is the unique stabilizing solution of the discrete-time Riccati equation

$$\mathbf{P} = \mathbf{APA}^T + \mathbf{BQB}^T - \mathbf{APR}_e^{-1}\mathbf{PA}^T, \tag{25}$$

and

$$\tilde{\mathbf{R}}_e = \sigma^2(\mathbf{I}_m + \tilde{\mathbf{P}}), \tag{26}$$

where $\tilde{\mathbf{P}}$ is the unique positive-semidefinite solution of the following Lyapunov equation

$$\tilde{\mathbf{P}} = (\mathbf{A} - \mathbf{K}_p)\tilde{\mathbf{P}}(\mathbf{A} - \mathbf{K}_p)^T + \mathbf{K}_p\mathbf{K}_p^T, \tag{27}$$

and $\mathbf{K}_p = \mathbf{APR}_e^{-1}$.

Proposition 2 is proved by extending the results in [17] with modification from scalar to vector observations.

Using (23), we now investigate the large sample detection performance for arbitrary periodic configuration. First, we consider the case of $M = 2$ in which we have freedom to schedule one intermediate sensor at an arbitrary location within an interval Δ. Periodic clustering and uniform configuration are special cases of this configuration with $\Delta_1 = 0$ and $\Delta_1 = \Delta/2$, respectively. Fig. 8

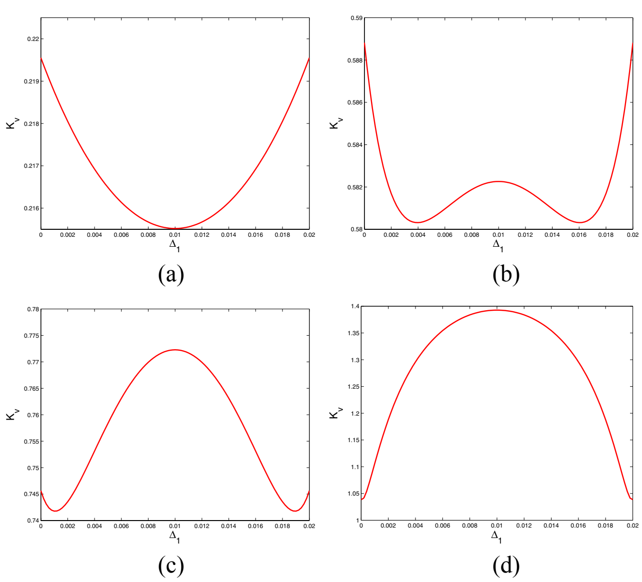

Fig. 8. K_v vs. Δ_1 ($M = 2$, $\Delta = 0.02$, SNR = 10 dB): (a) $A = 1$ (b) $A = 8$ (c) $A = 15$ (d) $A = 100$

shows the error exponent for different diffusion rates at high SNR. We observe an interesting behavior w.r.t. the diffusion rate. For the highly correlated field ($A = 1$), periodic clustering ($\Delta_1 = 0$) gives the best performance while uniform configuration provides the worst. However, as the field correlation becomes weak ($A = 8$), we observe a second lobe grow at the uniform configuration point ($\Delta_1 = \Delta/2$). The value of the second lobe becomes larger than that corresponding clustering as the correlation becomes weaker ($A = 15$), and eventually the error exponent decreases monotonically as the configuration deviates from uniform configuration to periodic clustering. This behavior of the error exponent clearly shows that the optimal configuration depends on the field correlation. Consistent with the results in the previous sections, one should reduce the correlation between observations for highly correlated fields while the uniform configuration is best for almost independent signal fields. Interestingly, the optimal configuration for $M = 2$ at high SNR is either the clustering or the uniform configuration depending on the field correlation; no configuration in-between is optimal! Fig. 9 shows the error exponent for $M = 2$ at low SNR. It is seen that clustering is always the best strategy for all values of field correlation considered since the increase in the effective SNR due to noise averaging is the dominant factor in detection performance at low SNR. It is also seen that the location of the intermediate sensor is not important for the highly uncorrelated field ($A = 1000$) unless it is very close to the first sensor within a period. This is intuitively obvious since the intermediate sensor provides an almost independent observation (for which the location does not matter) as it separates from the first and the noise averaging is not available between the independent samples.

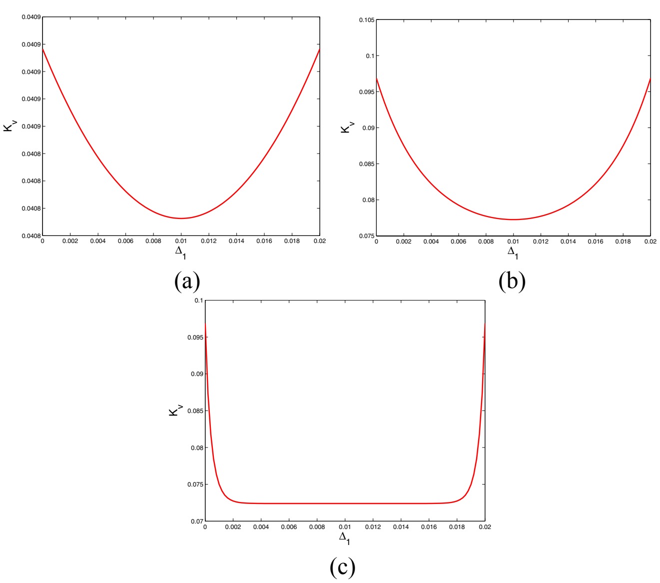

Fig. 9. K_v vs. Δ_1 ($M = 2$, $\Delta = 0.02$, SNR = -3 dB): (a) $A = 1$ (b) $A = 100$ (c) $A = 1000$

For the case of $M = 3$, due to the periodicity, the location of one sensor in a period is fixed and we can choose the locations (x_2, x_3) of the two other sensors arbitrarily such that $0 \leq x_2 \leq \Delta$ and $0 \leq x_3 \leq \Delta$. Fig. 10 shows the error exponent as a function of (x_2, x_3) for $M = 3$ at 10 dB SNR. Similar behavior is seen as in the case of $M = 2$. For the highly correlated signal ($A = 1$), we see the maximal value of the error exponent at $(0,0)$,$(0,\Delta)$,$(\Delta,0)$, and (Δ,Δ), which all correspond to periodic clustering. Hence, periodic clustering is the best among all configurations. In this case, it is seen that uniform configuration is the worst configuration. As the field correlation becomes weak, however, the best configuration moves to uniform configuration eventually, as seen in Fig 10 (d). It is seen that placing two sensors clustered and one in the middle of the

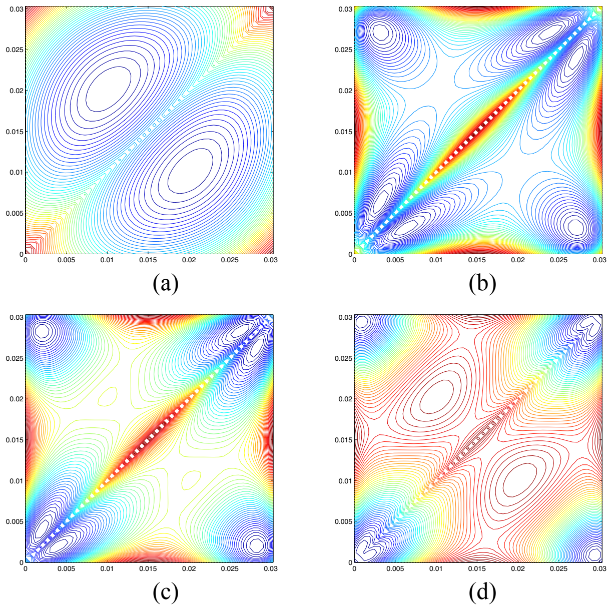

Fig. 10. K_v vs. (x_2, x_3) ($M = 3$, $\Delta = 0.03$, SNR = 10 dB): (a) $A = 1$ (b) $A = 5$ (c) $A = 6$ (d) $A = 9$ (red:high value, blue:low value)

spatial period is optimal for transitory values of field correlation as shown in Fig. 10 (b) and (c). Figure 11 summarizes the optimal configuration for different field correlation. Other results confirm that

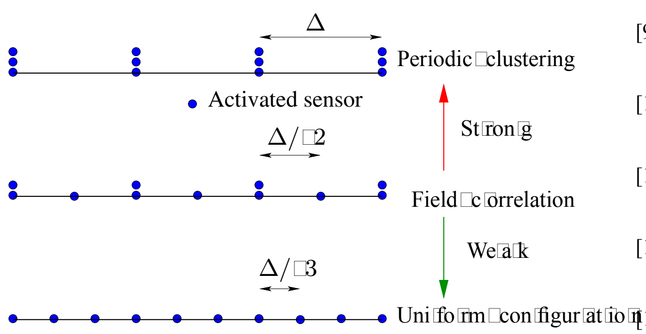

Fig. 11. Optimal configuration for $M = 3$ (SNR = 10 dB)

periodic clustering gives the best configuration for most values of field correlations at low SNR.

D. Sensor Placement

So far we have assumed that sensors have already been deployed and considered the activation for sensing and transmissions from the selected sensors. A related problem is sensor placement. When n sensors are planned to be deployed over a signal field for the detection application, how should we place the n sensors in the field? The results in the previous sections provide the answer for this problem as well.

IV. CONCLUSION

We have considered energy-efficient sensor activation for large sensor networks deployed to detect correlated random fields. Using our results on large-sample error behavior in this application, we have analyzed and compared the detection capabilities of different sensor configuration strategies. The optimal configuration is a function of the field correlation and the SNR of sensor observations. For uniform configuration, the scheduled sensors should be maximally separated to cover the entire signal field for SNR $>$ 1. For SNR $<$ 1, on the other hand, there exists an optimal spacing between the scheduled sensors. We have also derived the error exponents of periodic clustering and arbitrary periodic configuration. Periodic clustering may outperform uniform configuration depending on the field correlation and SNR. Furthermore, there exists an optimal cluster size for intermediate values of correlation. The closed-form error exponent obtained for the vector state-space model explains the transitory error behavior from periodic clustering to uniform configuration.

REFERENCES

[1] H. V. Poor, *An Introduction to Signal Detection and Estimation*, 2nd Edition, Springer, New York, 1994.

[2] C. W. Helstrom, *Elements of Signal Detection and Estimation*, Prentice-Hall, Englewood Cliffs, NJ, 1994.

[3] D. Cox and H. Miller, *The Theory of Stochastic Processes*, John Wiley & Sons Inc., New York, 1965.

[4] M. Micheli and M. I. Jordan, “Random sampling of a continuous-time stochastic dynamical system,” *Proc. of the 15th International Symposium on the Mathematical Theory of Networks and Systems (MTNS 2002),* (University of Notre Dame, South Bend, Indiana), August 2002.

[5] T. Kailath and H. V. Poor, “Detection of stochastic processes,” *IEEE Trans. on Information Theory*, vol. 44, no. 6, pp. 2230-2259, Oct. 1998.

[6] F. C. Schweppe, “ Evaluation of likelihood functions for Gaussian signals,” *IEEE Trans. on Information Theory*, vol.IT-1, pp.61-70, 1965.

[7] R. Gray, “On the asymptotic eigenvalue distribution of Toeplitz matrices,” *IEEE Trans. on Information Theory,* vol. 18, no. 6, pp. 725-730, Nov 1972.

[8] G. R. Benitz and J. A. Bucklew, “Large deviation rate calculations for nonlinear detectors in Gaussian noise,” *IEEE Trans. on Information Theory*, vol. 36, no. 2, pp.358-371, March 1990.

[9] R. K. Bahr, “Asymptotic analysis of error probabilities for the nonzero-mean Gaussian hypothesis testing problem,” *IEEE Trans. on Information Theory*, vol. 36, no. 3, pp.597-607, March 1990.

[10] R. K. Bahr and J. A. Bucklew, “Optimal sampling schemes for the Gaussian hypothesis testing problem,” *IEEE Trans. on Acoustics, Speech, and Signal Processing*, vol. 38, no. 10, pp.1677-1686, Oct. 1990.

[11] P. Barone, A. Gigli, and M. Piccioni, “Optimal importance sampling some quadratic forms of ARMA processes,” *IEEE Trans. on Information Theory,* vol. 41, no. 6, pp. 1834 - 1844, 1995.

[12] W. Bryc and W. Smolenski, “On the large deviation principle for a quadratic functional of the autoregressive process,” *Statistics and Probability Letters,* vol. 17, pp. 281-285, 1993.

[13] B. Bercu, F. Gamboa, and A. Rouault, “Large deviations for quadratic forms of stationary Gaussian processes,” *Stochastic Processes and their Applications,* vol. 71, pp. 75-90, 1997.

[14] H. Luschgy, “Asymptotic behavior of Neyman-Pearson tests for autoregressive processes,” *Scand. J. Statist.*, vol. 21, pp. 461-473, 1994.

[15] I. Vajda, *Theory of Statistical Inference and Information,* Kluwer Academic Publishers, Dordrecht, 1989.

[16] J.-F. Chamberland and V. V. Veeravalli, “Design of sensor networks for detection applications via large-deviation theory,” *Proc. 2004 IEEE Information Theory Workshop,* San Antonio, TX, Oct. 2004.

[17] Y. Sung, L. Tong, and H. V. Poor, “Neyman-Pearson detection of Gauss-Markov signals in noise: Closed-form error exponent and properties,” submitted to *IEEE Trans. on Information Theory*, Nov. 2004.

[18] Y. Sung, L. Tong, and H. V. Poor, “Sensor scheduling and activation for field detection in large sensor arrays,” preprint, Nov. 2004.